Journal of Heat and Mass Transfer Research

Journal homepage: https://jhmtr.semnan.ac.ir

Semnan University

ISSN: 2383-3068

Research Article

CFD Simulation of Photovoltaic Thermal (PV/T) Cooling System with Various Channel Geometries

I Gede Febri Bala Antara [a], Made Sucipta [a]*, Ketut Astawa [a], I Ketut Gede Wirawan [a], Made Sukrawa [b]

[a] *Mechanical Engineering Department of Udayana University, Street of Bukit Jimbaran, Badung, Bali 80361, Indonesia*

[b] *Civil Engineering Department of Udayana University, Street of Bukit Jimbaran, Badung, Bali 80361, Indonesia*

ARTICLE INFO

Article history:

Received: 2024-04-14

Revised: 2024-08-22

Accepted: 2024-08-22

Keywords:

Photovoltaic;

PV/T;

Cooling system;

Flow geometries;

Flow characteristics.

ABSTRACT

Photovoltaic/thermal (PV/T) is a solution for solar energy conversion devices to increase their efficiency. One of the challenges of PV/T is maintaining the temperature at optimal working conditions. Various studies have been conducted to improve PV/T performance, one of which is through the design of thermal collectors on PV/T. In this study, Computational Fluid Dynamics (CFD) simulations were conducted using four different types of channels: circular, hexagonal, semi-circular, and square. The channels were made with the same tube cross-sectional area and mass flow rate of 0.0016 m^2 and 0.0096 kg/s, respectively. The simulation results show that the circular channel numerically gives the lowest PV cell temperature, 317.95 K, with an electrical efficiency of 14.70% and a thermal efficiency of 44.18%. This is because the water velocity in the circular channel can be faster than the other channels. The circular channel has a thinner boundary layer, so the velocity is maximized, and the heat transfer rate increases.

1. Introduction

In recent decades, photovoltaic thermal (PV/T) has been widely developed due to its higher efficiency compared to the use of ordinary photovoltaic (PV) modules [1]. PV/T is PV combined with thermal collectors to increase its efficiency [2]. During midday, the intensity of solar radiation reaches its peak, decreasing PV performance [3]. Increasing the temperature of the PV will increase the electric current generated. Excessive current is less necessary because the voltage will decrease [4].

Many researchers have found the optimal working temperature of PV around 25°C [5]. However, in countries near the equator, the ambient temperature is higher than at the far end due to the ellipsoid shape of the earth. [6]. These conditions can reduce the performance of PV work if the heat received accumulates in PV cells. The thermal efficiency of PV/T is in the range of 28-45%, and the electrical efficiency is in the range of 10.6-12.2% [7, 8]. The decrease in cell efficiency is typically a 0.4% per °C increase in temperature [9]. If the temperature exceeds the acceptable capability (around 80°C), the PV cell will be damaged [10]. For this reason, the PV must be kept at its optimal working temperature. One of the steps that can be taken is to combine thermal collectors on PV. In addition to cooling,

* **Corresponding author.**
E-mail address: *m.sucipta@unud.ac.id*

Cite this article as:
Antara, I. G. F. B., Sucipta, M., Astawa, K., Wirawan, I. K. G. and Sukrawa, M., 2024. CFD Simulation of Photovoltaic Thermal (PV/T) Cooling System with Various Channel Geometries. *Journal of Heat and Mass Transfer Research*, 11(2), pp. 297-306.
https://doi.org/10.22075/JHMTR.2024.33787.1551

the heat from the cooling fluid (generally using water because its density and thermal conductivity are quite high and easy to obtain) can be reused as a household water heater on an industrial scale [11].

Some previous experiments have looked at replacing the coolant, and some have improved the channel design [12, 13]. Coolant replacement is done with liquids with higher thermal conductivity, usually ethylene glycol. However, using such fluids is unrealistic and requires expensive maintenance [14]. Another step that can be taken is to modify the water channel, such as the flow pattern, channel shape, or material used. The channel is the most influential factor in the heat transfer process [15]. There are other studies that vary the geometry of circular, rhombus, and elliptic, with results that the elliptic is the best and can produce 14.56% of electricity [16]. Some researchers have also compared several channel shapes, such as circular [15, 17, 18, 19], semi-circular [19, 20], and square [19]. A comparison of square and circular channels was carried out, resulting in circular geometry having a higher fluid flow rate [17, 18]. Other studies have also compared channels with circular, semi-circular, and square shapes. The results show that the semi-circular shape gives higher efficiency [19]. Another study compared squares, circles, and triangles, resulting in the triangle being the best because it gets the minimum temperature of 301.01 K when G is 1000 W/m^2 and the flow volume is 0.0005 m^3/s [21].

With these different experimental results, Computational Fluid Dynamics (CFD) simulations comparing PV cell channel geometries with circular, semi-circular, square, and hexagon shapes were conducted in this study. The simulation is controlled with the same cross-sectional area design and tube length. The simulation results will be reviewed in terms of the final temperature of the PV as well as the characteristics of the fluid flow.

2. Methods

2.1. Governing Equation

The simulations carried out in this study refer to the equilibrium equations. The results obtained are expected to represent the actual situation. The mass conservation equation, or what can be called mass conservation, is a fundamental principle that states that the total mass in a closed system is constant over time.

$$\frac{dM}{dt} = 0 \tag{1}$$

where dM is the change in mass while dt is the change in time.

Conservation of momentum is closely related to the Navier-Stokes equation, which states that the total momentum in a fluid system remains constant if no external force is acting on the system. The Navier-Stokes equation for incompressible fluids can be written as:

$$\rho\left(\frac{\partial v}{\partial t} + (v\nabla)v\right) = -\nabla p + \nabla\tau + \rho g \tag{2}$$

where ρ is the fluid density, v is the velocity vector, t is time, p is pressure, τ is the viscous stress tensor, and g is the gravitational acceleration.

The three-dimensional heat conduction equation describes the three-dimensional temperature distribution of solids against time. It is a partial differential equation that describes heat transfer through conduction. The general form of the 3D heat conduction equation in Cartesian coordinates is given by

$$\rho c\left(\frac{\partial T}{\partial t}\right) = \nabla(\mathrm{k}\nabla\mathrm{T}) + \mathrm{Q} \tag{3}$$

where ρ is the density of the fluid, c is the material's specific heat capacity, T is the temperature, t is the time, k is the thermal conductivity, and Q is the heat generation.

2.2. Model Design

The initial stage was modeling using Autodesk Inventor software. The model consists of three parts, namely the PV cell part, the absorbance part, and the fluid part. The PV cell is described as a plate with characteristics resembling a PV cell, with specifications shown in Table 1. The spiral flow shape (Fig. 1(a)) is used in this simulation because it is considered to be the most effective in conducting heat and this shape covers the entire surface area of the absorber plate. [22]. The arrangement of components from the top is a PV cell with an absorber plate at the bottom. The tube is attached directly to the absorber plate (Fig. 1(b)).

This simulation created four types of tube geometries: circular, semi-circular, square, and hexagonal. All variations are controlled with the same cross-sectional area of 0.0016 m^2 with each size shown in (Fig. 2). The length of the pipe, l is made the same as 18.9 m, with the thickness of the pipe made 0.003 m. The material used in the pipe is copper, which is directly attached to the absorbent plate. Each geometry's hydraulic diameter (D_h) will be different by making the same cross-sectional area. Each circular, hexagonal, semi-circular, and square channel has a D_h of 0.0381, 0.0399, 0.0390, and 0.0400 m, respectively.

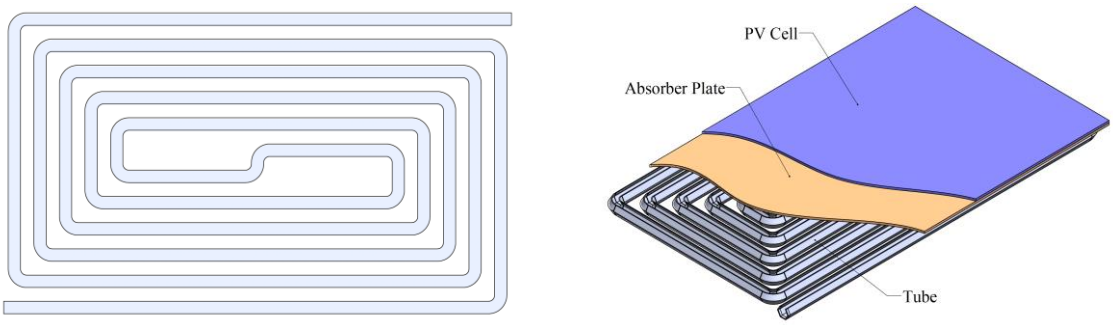

Fig. 1. PV/T experimental design model: (a) design of spiral channel fluid part and (b) PV/T model design component arrangement.

Table 1. PV/T Design Specifications

Component	Parameter	Value
PV Module [20]	Material	Monocrystalline
	L x W (m)	1.64 x 0.98
	Thickness, T (m)	0.005
	Thermal Conductivity, k (W/m. K)	148
	Density, ρ (kg/m^3)	2330
	Specific Heat Capacity, C_p (J/kg. K)	677
Absorber plate	Material	Copper
	L x W (m)	1.64 x 0.98
	Thickness, T (m)	0.005
	Thermal Conductivity, k (W/m. K)	401
	Density, ρ (kg/m^3)	8300
	Specific Heat Capacity, C_p (J/kg. K)	390

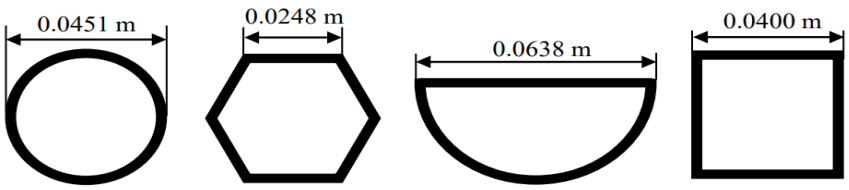

Fig. 2. Dimensions of PV/T tube

Inner diameter is used in tubes to equalise the cross-sectional area of all fluid channels. Through the law of conservation of mass, the mass flow rate is influenced by fluid density (in this case, the fluid used is water), cross-sectional area, and fluid flow velocity. By controlling the cross-sectional area to be the same, the temperature of the PV cell will be affected by the water velocity and density. The mass flow rate influences the convection heat transfer from the tube wall to the water. Thus, the effect of temperature on the PV cell can be seen from the velocity phenomenon in the tube.

This simulation follows the standard test condition (STC), defined as G at 1000 W/m^2 (1 kW/m^2) of midday sunlight when the PV cell is at a standard ambient temperature of 25°C. The boundary conditions in this simulation include convection heat transfer, h in the PV cell at 5 W/ m^2 °C, with constant heat received by the PV cell G at 1000 W/m^2. The ambient temperature is 298 K. No heat loss occurs in the PV, except convection. The PV cell fully absorbs the heat flux from the sun; in other words, the absorption capacity of the PV cell is assumed to be one. No contact resistance is taken between the PV and the absorber plate. The simulation model is a fluid-structure interaction (FSI) coupled system between water and tube walls. The four variations of the channel geometry are given the same initial mass flow rate of 0.0096 kg/s. Finally, the achieved electrical and thermal efficiency of the PV/T is considered to be the performance of this simulation.

2.3. PV/T Work Evaluation

For evaluation in this experiment, the following equations were used to determine the value of PV/T efficiency. To see the electric performance of PV/T, the following equation is used:

$$\eta_{elec} = \eta_{ref}\left[1 - \beta\left(T_{Cell} - T_{ref}\right)\right] \quad (4)$$

where η_{ref} is the efficiency of the PV module at the reference temperature [23], β = 0.0045 is the temperature coefficient [24]. T_{Cell} is the final temperature of the PV cell, and T_{ref} is the reference temperature of conventional PV of 25°C.

The thermal efficiency of PV/T can be reviewed through the following equation:

$$\eta_{th} = \frac{C_p \dot{m}\,(T_\infty - T_0)}{GA} \quad (5)$$

where C_p is the specific heat of the cooling fluid J(kg. K), $\dot{m}$ is the mass flow rate of the cooling fluid kg/s, G is the solar radiation W/m^2, A is the area of the PV/T collector m^2, T_0 and T_∞ are the initial temperature and outlet temperature of the water.

The overall efficiency of PV/T results from accumulating electric efficiency with thermal efficiency.

$$\eta_{overall} = \eta_{elec} + \eta_{thermal} \quad (6)$$

2.4. Meshing Evaluation

Meshing is done to facilitate the computational process by dividing the geometry into simpler elements. In addition, meshing affects the level of accuracy of the simulation model's conformity to actual conditions. In the meshing process, it is necessary to know the quality of the meshing to see the accuracy of the resulting solution. Meshing is done directly in ANSYS software (Fig. 3). It is important to consider the optimal number of elements to provide accurate and consistent results. Grid independency ensures that the simulation results do not depend on the size or density of the mesh used. In this simulation, a study on grid independency has been carried out which is shown in Fig. 4. From the experiments conducted, it has been found that the convergence point starts when the element number is 448,706 with a PV temperature reached 319.07 K when the element size is given 5 mm. At element sizes of 4 mm and 3 mm, the resulting temperatures are relatively the same, 319.07 and 319.08 K, respectively.

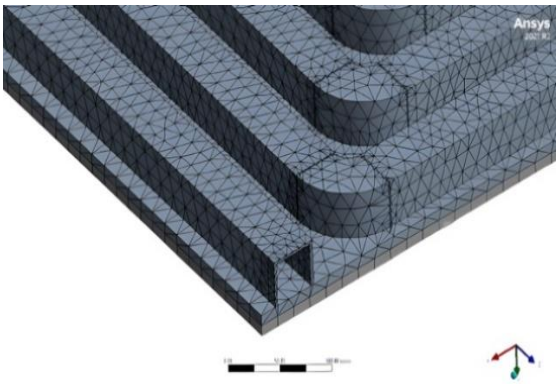

Fig. 3. Model mesh

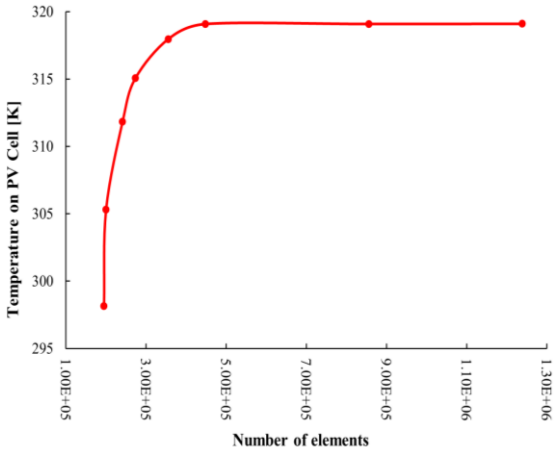

Fig. 4. Grid Independence study

Since the tube area is the same, the difference in the number of elements that occur in each tube is not significant. Therefore, in this simulation, an element size of 5 mm is chosen to simplify the numerical calculation process. The average number of nodes and elements of all channels are 673,816.75 and 446,278, respectively. The average quality of orthogonality was 0.72, and skewness was 0.27. These quality values are already in the "Very good" range on the metric spectrum (Fig. 5), so the model is suitable for simulation.

Skewness mesh metrics spectrum:

Excellent	Very good	Good	Acceptable	Bad	Unacceptable
0-0.25	0.25-0.50	0.50-0.80	0.80-0.94	0.95-0.97	0.98-1.00

Orthogonal Quality mesh metrics spectrum:

Unacceptable	Bad	Acceptable	Good	Very good	Excellent
0-0.001	0.001-0.14	0.15-0.20	0.20-0.69	0.70-0.95	0.95-1.00

Fig. 5. Mesh metrics spectrum [25].

3. Results and Discussion

The following section describes the results of the simulations carried out in this study.

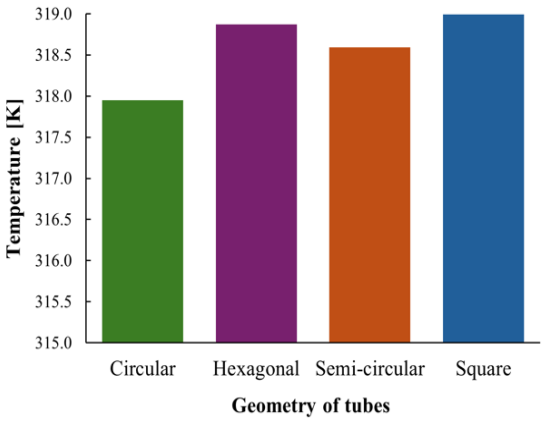

Fig. 6. Average temperature of the PV cell.

3.1. Temperature on PV Cells

The simulations carried out have followed the method described previously with reference to existing literature. The simulation results in Fig. 6 are four-channel variations that show the differences visually. The numerical results of the average temperature are used to describe the temperature distribution that occurs in the PV cell. The average temperature in the PV cell is presented using a bar graph shown in Fig. 6. The data is taken directly through ANSYS software.

The bar graph (Fig. 6) shows the lowest average temperature of PV cells with circular channel tubes. The lower the temperature, increasing the heat transfer in the PV cell. When compared, the circular channel is the best in this case, followed by the semi-circular, hexagonal, and square channels. When associated with the condition of the PV cell in Fig. 6 with the average temperature, the results correspond to the lowest temperature reached by the PV cell in the circular pipe with a dominant dark green temperature gradient (Fig. 7(a)). In contrast, the square tube (Fig. 7(d)) has many yellow gradients, indicating a high temperature. The average PV temperature in the circular channel is 317.95 K, while in the square channel it is 318.99 K. The semi-circular and hexagonal channels are 318.87 K and 318.59 K, respectively.

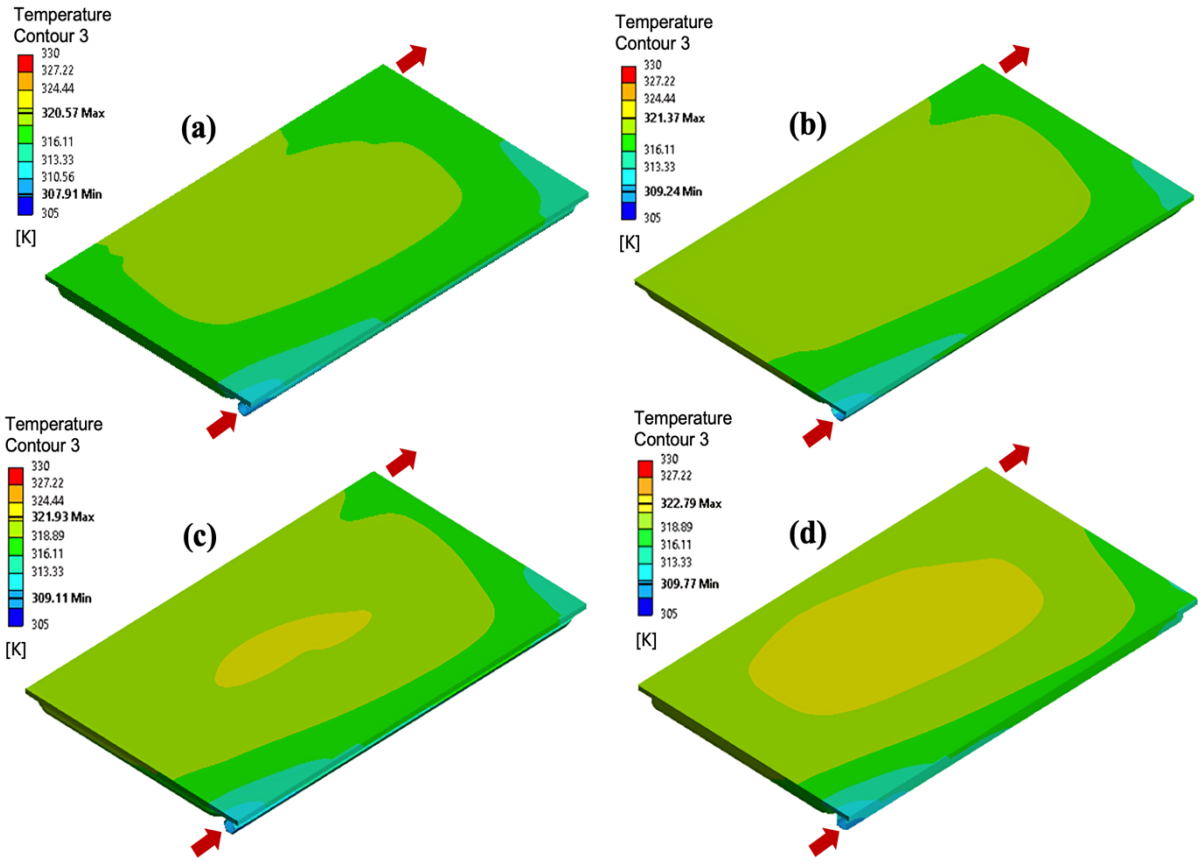

Fig. 7. Simulated temperature distribution of PV cells: (a) circular; (b) semi-circular; (c) hexagonal; (d) square.

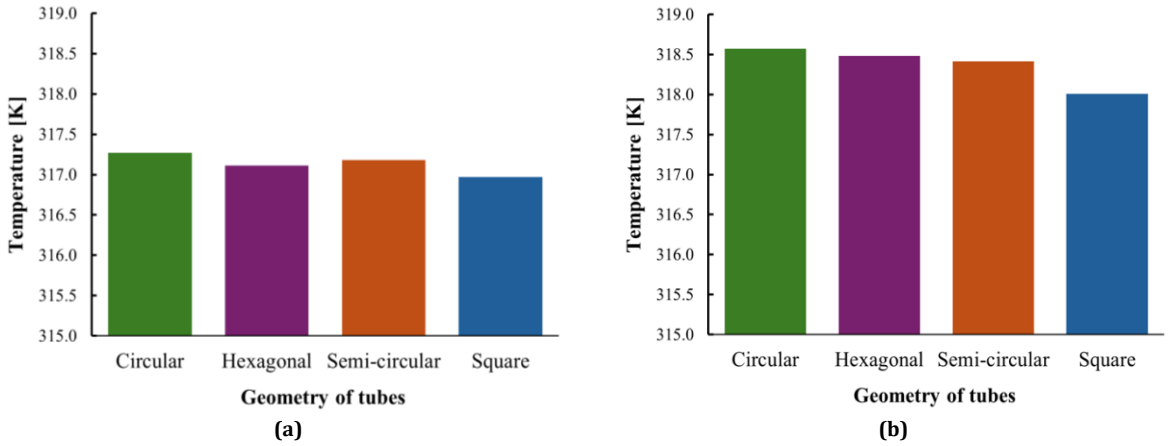

Fig. 8. (a) Average water temperature and (b) average water outlet temperature.

3.2. Cooling Water Condition

Temperature conditions in water need to be considered to see the ability of water to absorb heat from variations in channel geometry. The average water temperature (Fig. 8(a)) in the circular channel is the highest at 317.27 K. Furthermore, semi-circular, hexagonal, and square are 317.18 K, 317.11, and 316.97 K, respectively. If correlated with the temperature conditions in the PV cell (Fig. 7), the magnitude of the average water temperature is directly proportional to the temperature drop in the PV cell. The circular channel also has the highest water outlet temperature, 318.57 K. However, the semi-circular channel has a lower outlet temperature than the hexagonal, although, from the average water temperature, the semi-circular has a higher temperature than the hexagonal.

The difference between the two geometries is not much different between the hexagonal and semi-circular channels, which are 318.48 K and 318.41 K, respectively. However, when viewed from the outlet mass flow rate, the hexagonal channel has a higher mass flow rate of 0.0071870402 kg/s than the semi-circular channel of 0.0071638781 kg/s. The occurrence of unnoticeable temperature differences is due to the cross-sectional area that is kept the same, resulting in the magnitude of the convection value is relatively the same. This condition is in accordance with Lin's statement that the amount of convection is influenced by the heat transfer surface area [26]. The difference is caused by the varying channel shapes.

The insignificant temperature difference must be seen by comparing the velocity streamline in each channel. Fig. 9 shows the results of the velocity streamline viewed from the top view. Visually, it can be seen that the circular and semi-circular streamlines (Fig. 9(a) and Fig. 9(b)) have almost relatively the same line colour gradient. However, in the hexagonal and square channels (Fig. 9(c) and Fig. 9(d)), there are very many dark blue gradient lines, indicating that there are many low velocities in the water flow.

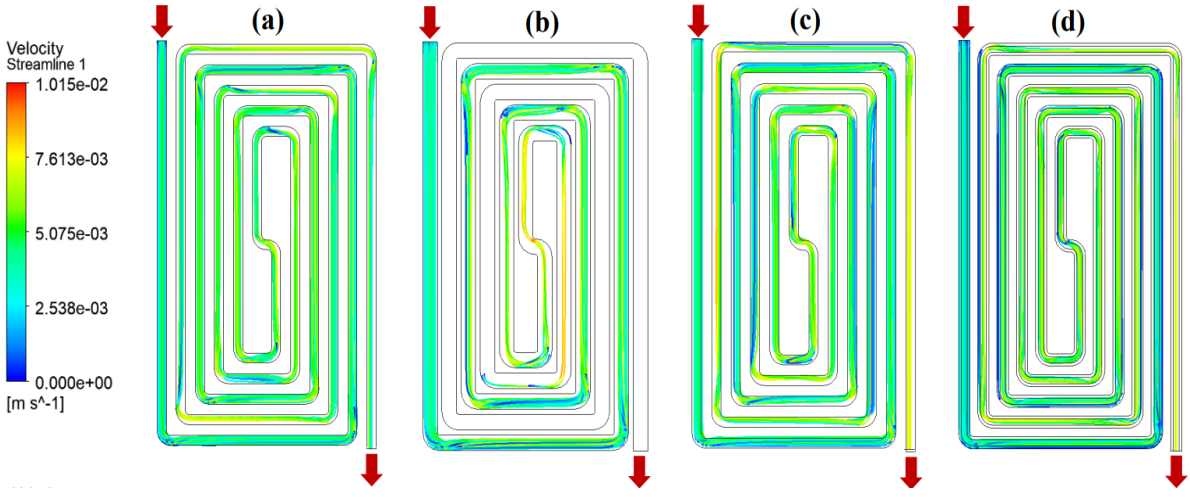

Fig. 9. Top view of water streamline velocity: (a) circular; (b) semi-circular; (c) hexagonal; (d) square.

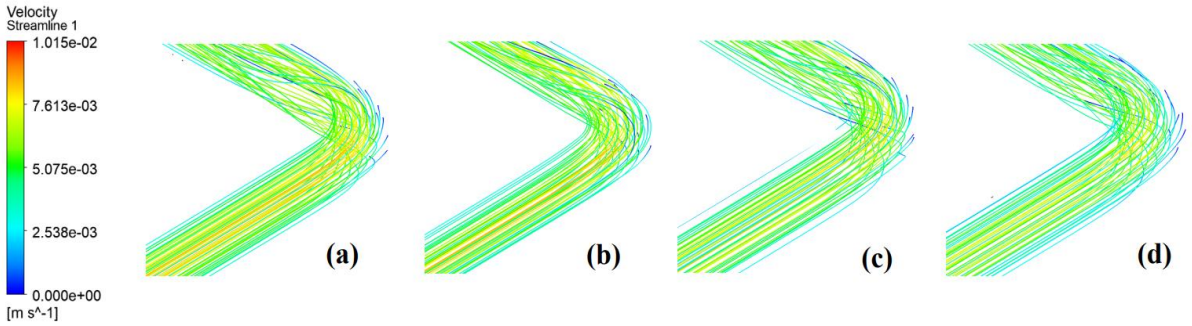

Fig. 10. Water streamline velocity section at the turn: (a) circular; (b) semi-circular; (c) hexagonal; (d) square.

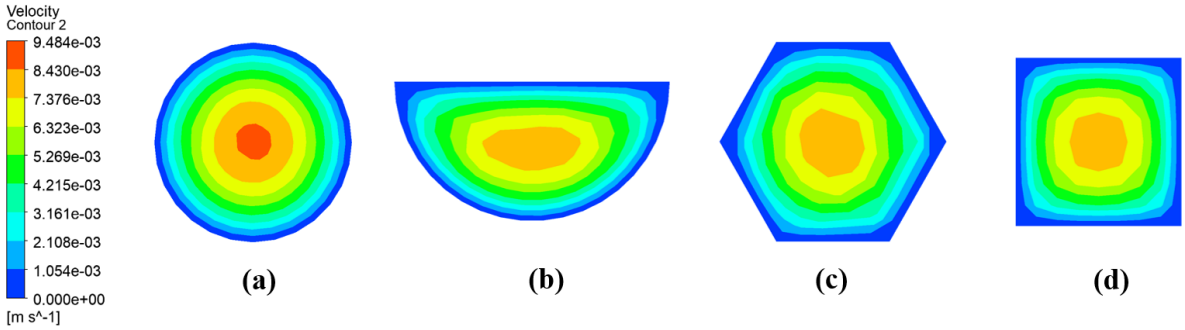

Fig. 11. Velocity distribution over the cross-sectional area of the PV/T channel: (a) circular; (b) semi-circular; (c) hexagonal; (d) square.

A closer look at the cut section of the turn reveals that the velocity of the circular channel (Fig. 10(a)) is predominantly red, indicating that the water velocity is quite high, unlike the square geometry (Fig. 10(d)) which is dominantly blue which indicates that the water velocity is relatively low. So, it can be concluded from the temperature conditions that occur in the PV cell and the temperature of the water that the faster the speed of the water in the channel pipe, the faster the heat transfer occurs. This is also in the context of convection heat transfer through fluid flow in the form of water; the faster the flow of water is, the more energetic the moving particles will be in transferring heat. Based on the temperature drop compared to the hydraulic diameter, it is in accordance with Hissouf et al. findings that the hydraulic diameter (D_h) affects the convection heat transfer coefficient between the working fluid and the tube wall. The smaller the D_h, the greater the heat transfer coefficient [19].

The velocity distribution over the cross-sectional area of the channel is shown in Fig. 11. Samples of the section are taken equally on all channels. It can be seen from the velocity contour that the circular channel has a thin boundary layer compared to other channels. In the square channel, it is clear that the contour with a thick dark blue colour indicates that the velocity in that area is zero. In contrast to the circular channel, the centre is red, indicating a higher maximum velocity than other channels.

3.3. Efficiency

As an evaluation of the simulation conducted, the electrical and thermal efficiency calculation is carried out by referring to the Eqs. (4-6) described in the methods section. Based on the bar graph in Fig. 12, it can be seen that the highest overall efficiency is achieved by the circular channel followed by semi-circular, hexagonal, and square.

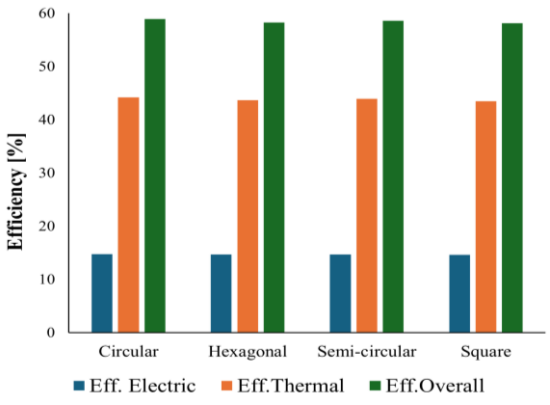

Fig. 12. Bar graph of efficiency at PV/T

The circular channel has the highest electric efficiency of 14.70%. Furthermore, the efficiency of semi-circular, hexagonal, and square are 14.65%, 14.63%, and 14.62%, respectively. Electric efficiency is affected by the average temperature of the PV cell. The lower the temperature on the PV cell, the more efficiency that occurs with reference to the STC reference

temperature. Furthermore, the highest thermal efficiency is in the circular channel at 44.18%, the semi-circular channel at 43.90%, the hexagonal at 43.64%, and the square at 43.46%.

The results of Baranwal et al. [20], who simulated the geometry of the PV/T cooling channel, suggested that the highest efficiency was found using a mass flow rate of 0.030 kg/s at 15.48%. The efficiency given is indeed higher but requires a high flow rate, which, of course, also increases the pump power. When viewed at the same mass flow rate in the study (about 0.0097 kg/s) with our simulation, the electrical efficiency that can be generated is 14.59% when G at 1000 W/m^2. When compared to the current simulation, the increase in electrical efficiency that occurs is not significant enough, but it is necessary to consider how the water flow conditions when given the same cross-sectional area with a minimum flow rate.

Another study by Sardouei et al [18] simulated 30, 60, 90, and 180 L/h of water flow with a circular cross section and found that the electrical efficiency of the same type in this simulation was 11.32% when given a flow rate close to that in this case of 30 L/h (0.0083 kg/s) when G at 1000 W/m^2.

This condition is in accordance with the results obtained by Emmanuel et al., who stated that the higher the temperature of the PV will reduce the electricity generated [17]. The inlet and outlet temperatures of the water influence thermal efficiency. The higher the outlet temperature of the tube in a PV/T system, the higher the thermal efficiency can be. This is because the temperature difference between the incoming and outgoing fluids affects the thermal energy efficiency. The study by Ewe et al. found that the highest thermal efficiency was recorded when the temperature difference between the outgoing and incoming fluids was the highest [27].

4. Conclusions

Photovoltaic thermal (PV/T) has recently undergone many developments to increase its efficiency. Thermal coupling of the collector helps to keep the PV temperature at its optimum working temperature. However, the temperature of PV that has been combined with thermal collectors still needs to be developed to get higher efficiency. In this experiment, a simulation using computational fluid dynamics (CFD) was carried out to see the performance of water flow in reducing the temperature of the PV cell through four variations of channel pipes: circular, hexagonal, semi-circular, and square. The settings given to the tubes include the same cross-sectional area and mass flow rate of 0.0016 m^2 and 0.0096 kg/s, respectively. From the results obtained, it can be concluded that the circular channel achieves the lowest temperature in the PV cell. The circular channel is better because the space utilisation on the channel is greater than that of other channels. This is evidenced by the boundary layer on the circular channel, which is thinner. The thinner the boundary layer formed, the higher the water velocity in the centre of the tube, and the heat resistance between the water and the pipe wall will be reduced so that the heat transfer becomes better. In contrast to the square channel, which has an angle, the corner experiences a significant decrease in velocity due to the whirlpool. The impact of a high-temperature drop on the PV cell will increase the water outlet temperature so that the thermal efficiency becomes higher. In addition, the size of the mass flow rate affects the amount of heat transfer that occurs. Electrical efficiency is influenced by the final temperature of the PV cell, the magnitude of which is 14.70%, 14.65%, 14.63%, and 14.62%, respectively, in circular, semi-circular, hexagonal, and square channels. The thermal efficiency achieved is 44.18%, 43.90%, 43.64%, and 43.46%, respectively.

Nomenclature

L	Length [m]
W	Width [m]
T	Thickness [m]
l	Length of tube [m]
D_h	Hydraulic Diameter [m]
k	Thermal Conductivity [W/m. K]
C_p	Specific Heat Capacity [J/kg. K]
M	Mass [kg]
t	Time [s]
v	Velocity [m/s]
g	Gravitational acceleration [m^2]
p	Pressure [Pa]
T	Temperature
$\dot{m}$	Mass flow rate [kg/s]
G	Solar radiation [W/m^2]
A	Area of PV [m^2]
h	Convective heat transfer coeff. [W/m^2 °C]
Q	Heat generation [J]

Greek Symbol

ρ	Density [kg/m^3]
∇	Divergence
τ	Viscous stress [Ns/m^2]
η	Efficiency [%]
β	Temperature Coeficient of PV

Acknowledgements

This research was supported/partially by the Thermofluids of Energy System and Material Research and Innovation Center (TESMRIC) Laboratory Mechanical Engineering. We thank our colleagues from Udayana University, who provided insight and expertise that greatly assisted the research.

Funding Statement

This research received no specific grant from funding agencies in the public, commercial, or not-for-profit sectors.

Conflicts of Interest

The author declares that there is no conflict of interest regarding the publication of this article.

References

[1] Abdul-Ganiyu, S., Quansah, D.A., Ramde, E.W., Seidu, R., Adaramola, M.S., 2020. Investigation of solar photovoltaic-thermal (PVT) and solar photovoltaic (PV) performance: A case study in Ghana. *Energies (Basel) 13* https://doi.org/10.3390/en13112701

[2] Diwania, S., Agrawal, S., Siddiqui, A.S. *et al.,* 2020. Photovoltaic–thermal (PV/T) technology: a comprehensive review on applications and its advancement. *Int J Energy Environ Eng 11*, 33–54. https://doi.org/10.1007/s40095-019-00327-y

[3] Budiyanto, M. A., & Lubis, M. H., 2020. Physical reviews of solar radiation models for estimating global solar radiation in Indonesia. *Energy Reports*, *6*, 1206-1211. https://doi.org/10.1016/j.egyr.2020.11.053

[4] Pavlovic, A., Fragassa, C., Bertoldi, M., Mikhnych, V., 2021. Thermal Behavior of Monocrystalline Silicon Solar Cells: A Numerical and Experimental Investigation on the Module Encapsulation Materials. Journal of Applied and Computational Mechanics 7, 1847–1855. https://doi.org/10.22055/jacm.2021.37852.3101

[5] Dwivedi, P., Sudhakar, K., Soni, A., Solomin, E., & Kirpichnikova, I., 2020. Advanced cooling techniques of PV modules: a state of art, Case Stud. Therm. *Eng. 21* (2020), 100674. https://doi.org/10.1016/j.csite.2020.100674

[6] Noxpanco, M. G., Wilkins, J., & Riffat, S., 2020. A review of the recent development of photovoltaic/thermal (Pv/t) systems and their applications. *Future Cities and Environment*, *6*, 9-9. https://doi.org/10.5334/fce.97

[7] Khanjari, Y., Pourfayaz, F., Kasaeian, A.B., 2016. Numerical investigation on using of nanofluid in a water-cooled photovoltaic thermal system. *Energy Convers Manag 122*, 263–278. https://doi.org/10.1016/j.enconman.2016.05.083

[8] Vajedi, H., Dehghan, M., Aminy, M., Pourrajabian, A. and Ilis, G.G., 2022. Experimental study on an air-based photovoltaic-thermal (PV-T) system with a converging thermal collector geometry: a comparative performance analysis. Sustainable *Energy Technologies and Assessments, 52*, p.102153. https://doi.org/10.1016/j.seta.2022.102153

[9] Yan, W. S., Tan, X. Y., Guan, L., Zhou, H. P., Yang, X. B., Xiang, P., & Zhong, Z. C., 2021. Solution of efficiency loss in thinned silicon PERC solar cells. *Renewable Energy*, *165*, 118-124. https://doi.org/10.1016/j.renene.2020.10.134

[10] Cotfas, D.T., Cotfas, P.A., Machidon, O.M., 2018. Study of temperature coefficients for parameters of photovoltaic cells. *International Journal of Photoenergy 2018*. https://doi.org/10.1155/2018/5945602

[11] Abdullah, A.L., Misha, S., Tamaldin, N., Rosli, M.A.M. and Sachit, F.A., 2020. Theoretical study and indoor experimental validation of performance of the new photovoltaic thermal solar collector (PVT) based water system. *Case Studies in Thermal Engineering, 18*, p.100595. https://doi.org/10.1016/j.csite.2020.100595

[12] Metwally, H., Mahmoud, N. A., Aboelsoud, W., & Ezzat, M., 2022. A critical review of photovoltaic panels thermal management: criteria and methods. *ASM*, *2*, 2.

[13] Pathak, S. K., Sharma, P. O., Goel, V., Bhattacharyya, S., Aybar, H. Ş., & Meyer, J. P., 2022. A detailed review on the performance of photovoltaic/thermal system using various cooling methods. *Sustainable Energy Technologies and Assessments*, *51*, 101844. https://doi.org/10.1016/j.seta.2021.101844

[14] Pang, W., Cui, Y., Zhang, Q., Yu, H., Zhang, L., Yan, H., 2019. Experimental effect of high mass flow rate and volume cooling on performance of a water-type PV/T collector. *Solar Energy, 188*, pp.1360–1368. https://doi.org/10.1016/j.solener.2019.07.024

[15] Kazem, H.A., Al-Waeli, A.H.A., Chaichan, M.T., Al-Waeli, K.H., Al-Aasam, A.B., Sopian, K., 2020. Evaluation and comparison of different flow configurations PVT systems in Oman: A numerical and experimental investigation. *Solar Energy, 208*, pp.58–88. https://doi.org/10.1016/j.solener.2020.07.078

[16] Khalili, Z., Sheikholeslami, M., & Momayez, L., 2023. Hybrid nanofluid flow within cooling tube of photovoltaic-thermoelectric solar unit. *Scientific Reports*, *13*(1), p.8202. https://doi.org/10.1038/s41598-023-35428-6

[17] Emmanuel, B., Yuan, Y., Gaudence, N. and Zhou, J., 2021. A review on the influence of the components on the performance of PVT modules. *Solar Energy, 226*, pp.365-388. https://doi.org/10.1016/j.solener.2021.08.042

[18] Sardouei, M.M., Mortezapour, H., Naeimi, K.J., 2018. Temperature distribution and efficiency assessment of different PVT water collector designs. Indian Academy of Sciences Sādhanā, 43, pp.1-13. https://doi.org/10.1007/s12046-018-0826-xS

[19] Hissouf, M., Feddaoui, M., Najim, M., Charef, A., 2020. Performance of a photovoltaic-thermal solar collector using two types of working fluids at different fluid channels geometry. *Renew Energy 162*, 1723–1734. https://doi.org/10.1016/j.renene.2020.09.097

[20] Baranwal, N.K. and Singhal, M.K., 2021. Modeling and simulation of a spiral type hybrid photovoltaic thermal (PV/T) water collector using ANSYS. In Advances in Clean Energy Technologies: Select Proceedings of ICET 2020 (pp. 127-139). Springer Singapore. https://doi.org/10.1007/978-981-16-0235-1_10

[21] Arifin, Z., Prasetyo, S.D., Prabowo, A.R., Tjahjana, D.D.D.P., Rachmanto, R.A., 2021. Effect of thermal collector configuration on the photovoltaic heat transfer performance with 3D CFD modeling. *Open Engineering 11*, 1076–1085. https://doi.org/10.1515/eng-2021-0107

[22] Tirupati Rao, V., & Raja Sekhar, Y., 2023. Hybrid photovoltaic/thermal (PVT) collector systems with different absorber configurations for thermal management–a review. *Energy & Environment*, *34*(3), pp. 690-735. https://doi.org/10.1177/0958305X211065575

[23] Popovici, C.G., Hudişteanu, S.V., Mateescu, T.D., Cherecheş, N.C., 2016. Efficiency Improvement of Photovoltaic Panels by Using Air Cooled Heat Sinks, in: Energy Procedia. Elsevier Ltd, pp. 425–432. https://doi.org/10.1016/j.egypro.2015.12.223

[24] Zondag, H. A., De Vries, D. D., Van Helden, W. G. J., van Zolingen, R. C., & Van Steenhoven, A. A., 2002. The thermal and electrical yield of a PV-thermal collector. *Solar energy*, *72*(2), 113-128. https://doi.org/10.1016/S0038-092X(01)00094-9

[25] ANSYS Inc, 2010. Ansys Meshing User's Guide.

[26] Lin, J., Hong, Y., & Lu, J., 2022. New method for the determination of convective heat transfer coefficient in fully-developed laminar pipe flow. *Acta Mechanica Sinica*, *38*(1), p.321430. https://doi.org/10.1007/s10409-021-09024-x

[27] Ewe, W.E., Fudholi, A., Sopian, K. and Asim, N., 2021. Modeling of bifacial photovoltaic-thermal (PVT) air heater with jet plate. *Int. J. Heat Technol, 39(4)*, pp.1117-1122. https://doi.org/10.18280/ijht.390409